CO Adsorption Site Preference on Platinum: Charge Is the Essence

G. T. Kasun Kalhara Gunasooriya[ORCID] and Mark Saeys*[ORCID]

Laboratory for Chemical Technology, Ghent University, Technologiepark 914, 9052 Gent, Belgium

S *Supporting Information*

ABSTRACT: The adsorption of CO on transition-metal surfaces is a key step in catalysis and a reference system for surface science and computational catalysis. Here, the change in CO site preference with coverage, from top to bridge and back to top, is analyzed using charge transfer and chemical bonding. The relative stability of top and bridge sites is related to the variation in the surface platinum charge with CO coverage. Both the Pt−C σ^* (Pauli repulsion) and the C−O π^* (back-donation) occupancies increase with platinum charge; however, destabilizing Pauli repulsion dominates over stabilizing back-donation, and adsorption weakens with increasing surface charge. CO at the top sites is more sensitive to Pauli repulsion, leading to a change in site preference from top to bridge with increasing platinum charge and, consequently, with increasing CO coverage. The higher back-donation at the bridge sites eventually switches the site preference back to top near monolayer coverage.

KEYWORDS: *catalysis, density functional theory, platinum, CO adsorption, site preference*
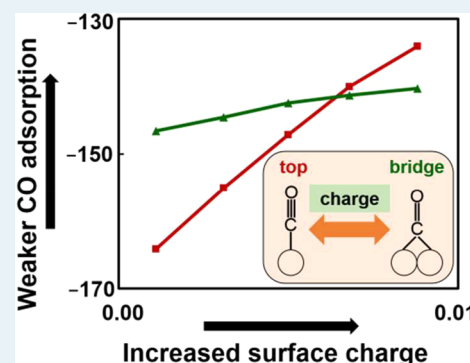
The adsorption of CO on transition-metal surfaces is an important model system for computational and experimental catalysis, and a crucial step in CO oxidation, water−gas shift, and Fischer−Tropsch Synthesis.[1,2] CO adsorption on platinum is often used as a bellwether system for surface science and computational catalysis, and has been studied with a wide range of experimental techniques. Surprisingly, the correct description of both the site preference and the adsorption energy remain important challenges for density functional theory (DFT),[3−7] and the origin of the change in site preference from top to bridge and back to top with coverage has not been fully understood.

At low coverage, experimental heats of adsorption range from −130 ± 3 kJ/mol for single-crystal adsorption calorimetry[8] to −138 ± 8 kJ/mol for work function measurements,[9] and −145 ± 15 kJ/mol for temperature-programmed desorption.[10] At low coverages, CO adsorbs preferentially at top sites, characterized by a sharp IR peak near 2100 cm^{-1}.[9,10] This site preference is also seen in low energy electron diffraction (LEED) studies at 300 K and for an exposure of 1 L.[9,10] Papp and Steinrück[11] showed that, in the limit of very low CO pressures, the site exchange flux between top and bridge sites is much higher than the adsorption flux, and the site occupations are hence close to thermal equilibrium. Using temperature-dependent adsorption experiments, it was then possible to determine an adsorption energy difference of 4 kJ/mol between CO at top and bridge sites.[12] For higher coverage, a distinct change in site preference is observed. At 0.5 ML, LEED studies show a well-ordered $c(4 \times 2)$ pattern.[10] Electron energy loss spectroscopy (EELS), reflection absorption infrared spectroscopy (RAIRS), He scattering, and X-ray photoemission spectroscopy (XPS) all demonstrate that CO adsorbs at both the top and bridge sites for this coverage.[10,13−17] The change in site preference from

top to bridge with increase in CO coverage on Pt surfaces is remarkable.

A similar change in site preference has been observed on other transition metals. At low CO coverage, CO adsorbs at the top sites, forming an ordered $(\sqrt{3} \times \sqrt{3})R30°−$CO structure on the (111) facets of Rh[18] and Ir[19] and on the (0001) facets of Co[20] and Ru.[21] For a higher CO coverage, CO adsorbs both on top and bridge sites, forming a $(2\sqrt{3} \times 2\sqrt{3})R30°−7$CO structure on Ir(111),[19] Co(0001),[20] and Ru(0001).[21] The origin of this change in site preference with coverage and an analysis of the electronic and chemical bonding factors that drive this change remain open questions.

Here, CO adsorption on Pt(111) was studied using periodic density functional theory with the vdW−DF,[22,23] PBE,[24] and BEEF−vdW[25] functionals as implemented in the Vienna Ab initio Simulation Package (VASP).[26,27] The Pt(111) surface was modeled as a five−layer slab using $p(3 \times 3)$ (for low coverage) and $c(4 \times 2)$ (for high coverage) unit cells. To evaluate the thermodynamic stability of the different structures, Gibbs free adsorption energies, ΔG_{ads} (300 K, 1 mbar), were calculated. Chemical bonding was analyzed using the periodic implementation of Natural Bond Orbitals (NBO) theory[28,29] and the Crystal Orbital Hamilton Population (COHP).[30,31] Bader charges[32] were computed to evaluate the effect of charge (see Supporting Information).

As shown in Table 1, vdW−DF correctly predicts the preference for the top site at low CO coverage, with an adsorption energy of −147 kJ/mol. This is slightly stronger than the experimental values, −130 to −145 kJ/mol.[8−10] CO
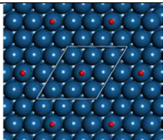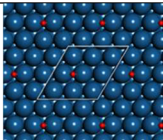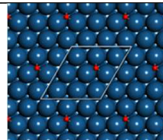
Table 1. CO Adsorption Energies (kJ/mol), Gibbs Free Adsorption Energies (300 K, 1 mbar CO) (kJ/mol), and CO Adsorption Entropies (J/mol K) for Different Low-Coverage Adsorption Sites on Pt(111)[a]

Functional	1/9 – 1T	1/9 – 1B	1/9 – 1H
vdW–DF	**−147**/−80/46	−143/−75/42	−139/−72/41
PBE	−174/−106/46	**−181**/−113/41	**−182**/−113/37
BEEF–vdW	−148/−80/47	**−152**/−84/41	−150/−82/39
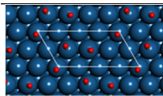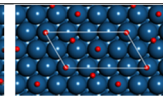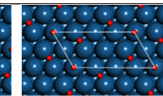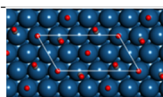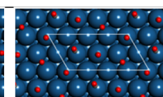
[a]The most stable adsorption site for each functional is indicated. (T, top; B, bridge; H, hollow).

Table 2. Average CO Adsorption Energies (kJ/mol), Average Gibbs Free Adsorption Energies (300 K, 1 mbar) (kJ/mol), and Average CO Adsorption Entropies (J/mol K) for Different High-Coverage Structures in a $c(4 \times 2)$ Unit Cell Obtained with the vdW–DF Functional[a]

3/8 – 3T	3/8 – 2T+1B	3/8 – 1T+2B
−135/−68/49	**−141**/−73/45	−138/−70/43
1/2 – 4T	**1/2 – 3T+1B**	**1/2 – 2T+2B**
−127/−60/49	−135/−67/46	**−139**/−70/43
1/2 – 1T+3B	**1 – 8T**	**1 – 8B**
−132/−63/42	**−77**/−4/31	−57/16/29

[a]The most stable configuration for each coverage is indicated (T, top; B, bridge).

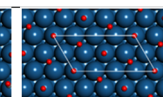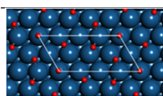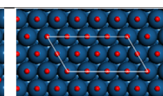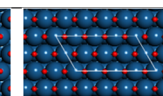adsorption at the bridge site is 5 kJ/mol less stable, a value that agrees well with the experimental energy difference between the top and the bridge site.[12] Adsorption at the hollow site is the least stable. This trend remains when the experimental lattice constant of 3.912 Å is used in the calculations, rather than the optimized lattice constant of 4.028 Å (Supporting Information Table S3). The PBE functional yields much stronger adsorption energies, especially for the hollow site, as is well documented.[3−7] The BEEF–vdW and the vdW–DF functional give similar adsorption energies, but the bridge and hollow site are preferred by BEEF–vdW. The energy difference between the three sites is however within the Bayesian error estimate for the BEEF–vdW values, 3 kJ/mol. The Gibbs free adsorption energy is very favorable for CO on Pt(111) at 300 K and 1 mbar CO. The entropy for CO at the top site is 4 J/(mol K) higher than for CO on the bridge and hollow sites. This higher entropy results from a higher frustrated translational entropy of 34 J/(mol K) compared to 29 J/(mol K) for the bridge site. Despite the stronger adsorption, CO is hence slightly more mobile at the top site. The preference of the bridge over the hollow site on Pt(111) agrees with experimental data, but this relative stability depends on the transition metal. On Co(0001), adsorption at the bridge site is 4 kJ/mol less stable than adsorption at the hollow site.[33,34] Indeed, CO adsorption at hollow sites is not observed on Pt(111), while it has been reported for high−coverage structures on Co(0001).[33,35]

Table 2 summarizes calculations using the vdW–DF functional for 3/8, 1/2 and 1 ML. Different combinations of bridge and top adsorption were considered in the $c(4 \times 2)$ unit cell (Table 2 and Supporting Information Table S4). At 1/2 ML, the most stable structure has an equal population of the top and the bridge sites, in agreement with XPS, RAIRS, EELS, and LEED data.[10,13−17] The structure with all CO at top sites is 12 kJ/mol less stable. Also at 3/8 ML, the bridge sites begin to be populated, illustrating the change in site preference with coverage.

To analyze the change in site preference with coverage, the Blyholder model[36,37] is used. The Blyholder model describes CO adsorption on transition metals as a balance between donation from the occupied CO 5σ molecular orbital to partially filled metal surface d-states and back-donation from occupied metal surface d-states to the empty CO $2\pi^*$ orbitals. For CO adsorption at the top site, the nonbonding CO 5σ molecular orbital (a lone pair on C) interacts with the partially filled metal d_{z^2} states. The metal d_{z^2} states broaden and split

into 5σ–d_{z^2} bonding states well below the Fermi level and partially filled 5σ–d_{z^2} antibonding states located around the Fermi level, as illustrated by the COHP density of states in Supporting Information Figure S2. The filling of this 5σ–d_{z^2} antibonding states indicates the strength of the Pauli repulsion between the occupied CO 5σ molecular orbital and the partially filled metal surface d-states.[38] At the bridge and hollow sites, the states resulting from the interaction between the CO 5σ orbital and the metal d-states are at a higher energy, indicating a weaker interaction (Supporting Information Figure S2), consistent with the longer Pt−C distance at these sites. The CO $2\pi^*$ molecular orbital interacts with metal d_{xz} and d_{yz} states for CO adsorption on top, bridge and hollow sites. Back-donation from occupied metal surface states to the empty CO $2\pi^*$ orbitals stretches the C−O bond and strengthens CO adsorption. The more detailed Pettersson−Nilsson model[39] includes additional MOs to describe the interaction between CO and metal surfaces.

The change in Pauli repulsion and in back-donation can be quantified by the occupancies of the corresponding Natural Bond Orbitals (NBOs) (Table 3 and Figure 1b). NBO analysis provides a localized chemical bonding description, based on familiar Lewis structures (Supporting Information Table S2). While the Pt−C σ, C−O σ and C−O π orbitals are essentially doubly occupied with occupancies above 1.9 electrons, the corresponding anti-bonding orbitals are also significantly filled and determine the stability and the site preference. The NBO occupancy of Pt−C σ^* is used as a measure of the Pauli repulsion between the occupied CO 5σ molecular orbital and the partially filled metal surface d-states. At low coverage (1/8 ML), the Pt−C σ^* NBO at the top site contains 0.530 electrons, while the 2 Pt−C σ^* NBOs at the bridge site contain 0.482 electrons each (Table 3). Back-donation to the CO $2\pi^*$ orbitals can be quantified from the occupancy of the C−O π^* NBOs. At low coverage, the C−O π^* NBO contains 0.198 electrons at the top site and 0.201 electrons the bridge site. The NBO occupancies of additional orbitals described in the Pettersson−Nilsson model however change very little with

Table 3. Differential CO Adsorption Energies for Top and Bridge Sites at 1/8 ML and 3/8 ML Coverage, and NBO Occupancy of the Pt−C σ* and of the C−O π* NBOs^a

NBO occupancy (electrons)	1/8 ML		3/8 ML	
	top	bridge	top	bridge
Pt−C σ*	0.530	0.482, 0.482	0.539	0.484, 0.484
C−O π*	0.198, 0.198	0.224	0.201, 0.201	0.232

^{a}Change in the Pt(111)−c(4 × 2) surface Bader charges (charge difference compared to clean slab) before CO adsorption (orange: the platinum atoms which CO adsorbs) and differential adsorption energies (in green) are shown.
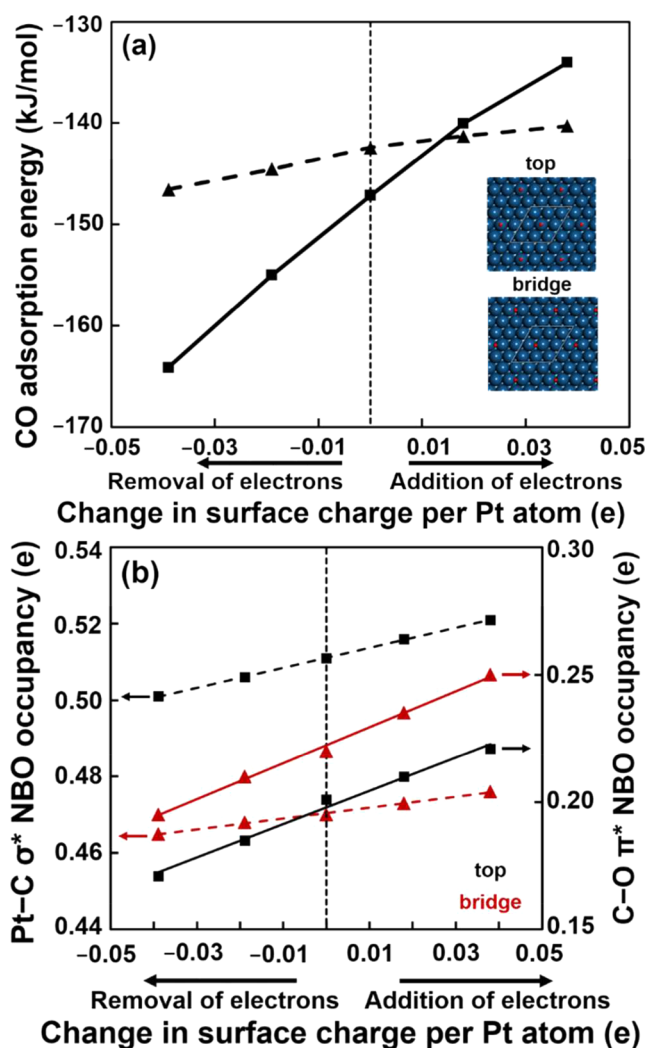

Figure 1. (a) Effect of Pt charge on the CO adsorption energy for top (■) and bridge (▲) sites at 1/9 ML coverage; (b) Effect of Pt charge on the Pt−C σ* NBO (dotted line) and the C−O π* NBO (solid line) occupancy for the top (■) and the bridge (▲) site.

charge (Supporting Information Table S6), and we therefore use the simpler Blyholder model to analyze the observed trends.

The occupancies of the Pt−C σ* NBOs and of the C−O π* NBOs are very sensitive to the charge of the surface Pt atoms. By tuning the charge of the surface Pt atoms (e.g., by adding electrons to the slab, by introducing electropositive or electronegative elements on the surface or by introducing an external electric field perpendicular to the surface), we can evaluate the relation between the Pt surface charge and the site preference. Figure 1a demonstrates that CO adsorption at the top site is more sensitive to the surface charge than CO adsorption at the bridge site (Supporting Information Table S5). Adsorption weakens both at the top and at the bridge site when Pt atoms become more negatively charged. Note that this trend is opposite to what is typically reported in homogeneous catalysis[40] and sometimes assumed in heterogeneous catalysis.[41] For the neutral surface, indicated by the dotted line in Figure 1a, the top site is 4 kJ/mol more stable than the bridge site. An increase in the Pt charge by only 0.015 electrons switches the preference to the bridge site. As we show below, such changes in surface charge can easily result from charge transfer upon adsorption. Figure 1b shows that the Pauli repulsion at the top site is twice as sensitive to the Pt charge as the Pauli repulsion at the bridge site. Indeed, the Pt−C bond at the top site stretches more for an increase in the Pt charge than the Pt−C bonds at the bridge site. This can be understood from the more directional interaction between the d_{z^2} states and the 5σ orbital at the top site. The increase in surface charge also increases back-donation to the C−O π* NBO, but the sensitivity for the top and the bridge site is similar. The effect of the surface charge on the adsorption energy and the site preference was confirmed by PBE calculations (Supporting Information Table S7). The occupancies of the C−O σ and the C−O π NBOs and of the O lone pair do not change significantly in response to the Pt surface charges (Table S6 and Figure 1b). In all cases, the adsorption energy correlates with the surface charge. For a given charge, we find a similar change in adsorption energy, whether induced by an electrostatic field or by the addition/removal of electrons.

The change in site preference with coverage can be understood from their different sensitivity to Pauli repulsion. For 1/8 ML, CO prefers the top site over the bridge site, with a difference of 3 kJ/mol (Table 3). However, the third CO in the c(4 × 2) unit cell preferentially adsorbs at the bridge site (Table 2). When CO adsorbs at the top site, there is a net charge transfer of 0.03 electrons from the Pt(111) surface to CO, and the Pt atom to which CO is bound loses 0.19 electrons. This

causes a charge redistribution on the Pt surface, leading to a *higher* electron density at the empty surface Pt atoms (Table 3). This 0.01 electron increase in the charge density at the neighboring Pt atoms (Table 3) significantly destabilizes CO adsorption at the top site. An atom-projected density of states (PDOS) analysis (Supporting Information Figure S4) illustrates that the charge increase results from a change in the occupancy of the d_{z^2} states. The interaction between the 5σ orbital and the partially filled d_{z^2} states seems to push electron density to the neighboring Pt atoms. The occupancy of the d_{xz} and d_{yz} states on the neighboring Pt atom changes by less than 0.005. It is important to note that a 0.01 electron change in Pt surface charge is significant and has a strong influence on the adsorption energy.[28] At the bridge site, the effect of Pauli repulsion is smaller and the increased back-donation (by 0.08 electron) increases the adsorption energy. While through space repulsion is slightly smaller for the latter structure (1–2 kJ/mol), the dominant factor is the surface Pt charge. The charge transfer to CO is more significant at the bridge site (0.13 electron at the bridge site vs 0.03 electron at the top site, Supporting Information Table S2). This difference in charge transfer for the top and the bridge site agrees with work function measurements.[9,10] For low coverages, the work function decreases with coverage because CO adsorption at the top sites raises the Fermi level. For higher coverages, the work function increases with CO coverage because increased back-donation at the bridge sites reduces the Fermi level.

When the coverage is increased to 1 monolayer, adsorption at the top site is again preferred by 20 kJ/mol (Table 2). The change in site preference at monolayer coverage stems from the higher back-donation for CO at the bridge sites. As shown in Figure 1a, removal of electrons from Pt favors CO adsorption at the top site. This charge sensitivity is also found at monolayer coverage: increasing the Pt charge by 0.233 electrons switches the preference to the bridge sites.

In conclusion, the vdW−DF functional correctly describes the site preference for CO on Pt(111), both at low, intermediate, and high coverage, resolving the so-called CO puzzle.[3] The change in site preference from top to bridge and back to top with increasing coverage is caused by the charge redistribution on the Pt surface upon CO adsorption. The directional metal d_{z^2}−CO 5σ interaction renders CO adsorption at the top site more sensitive to the surface charge than CO adsorption at the bridge or hollow site. In combination with a different balance between donation and back-donation, this higher sensitivity governs the change in site preference with coverage. Because the surface charge of Pt catalysts can be tuned by the support[42−44] or by promoters,[45,46] and the reactivity of CO depends on the adsorption site, charge provides a promising handle to tune the activity and selectivity of Pt catalysts.

■ ASSOCIATED CONTENT

Ⓢ Supporting Information

The Supporting Information is available free of charge on the ACS Publications website at DOI: 10.1021/acscatal.8b00214.

> (1) Computational methods; (2) CO adsorption sites on a Pt(111) catalyst surface; (3) COHP plots for CO molecule in gas phase, CO adsorbed on a top, bridge and hollow sites for 1/9 ML CO coverage; (4) COHP plots for CO adsorbed on a top and a bridge sites for 1/9 ML CO coverage with variation in the surface platinum

charge; (5) atom-projected density of states (PDOS) surface Pt atoms; (6) planar averaged electrostatic potential along the normal axis for clean neutral and clean charged slabs; (7) C−O and Pt−C bond lengths (Å), CO stretch frequency (cm^{-1}), occupancy of the Pt−C σ^* NBO and of the C−O π^* NBO, change in charge of the CO molecule upon adsorption for low-coverage CO structures; (8) low-coverage vdW−DF CO adsorption energy with optimized and experimental lattice constants; (9) low-coverage vdW−DF and PBE CO adsorption energies as the charge of the surface Pt atoms changes; (10) change in the occupancy of various NBOs for CO adsorption at the top and the bridge site as a function of the charge of the surface Pt atoms; and (11) vdW−DF frequencies of adsorbed CO for different configurations and coverages (PDF)

■ AUTHOR INFORMATION

Corresponding Author

*E-mail: mark.saeys@ugent.be.

ORCID

G. T. Kasun Kalhara Gunasooriya: 0000-0003-1258-7841
Mark Saeys: 0000-0002-3426-6662

Notes

The authors declare no competing financial interest.

■ REFERENCES

(1) Santen, R. A. *Modern Heterogeneous Catalysis*; Wiley-VCH Verlag GmbH & Co. KGaA: Weinheim, 2017; pp 15−58.

(2) Chorkendorff, I.; Niemantsverdriet, J. W. *Concepts of Modern Catalysis and Kinetics*, 2nd ed.; Wiley-VCH: Weinheim, 2007; pp 301−348.

(3) Feibelman, P. J.; Hammer, B.; Nørskov, J. K.; Wagner, F.; Scheffler, M.; Stumpf, R.; Watwe, R.; Dumesic, J. The CO/Pt(111) Puzzle†. *J. Phys. Chem. B* **2001**, *105*, 4018−4025.

(4) Kresse, G.; Gil, A.; Sautet, P. Significance of single-electron energies for the description of CO on Pt(111). *Phys. Rev. B: Condens. Matter Mater. Phys.* **2003**, *68*, 073401.

(5) Hu, Q.-M.; Reuter, K.; Scheffler, M. Towards an Exact Treatment of Exchange and Correlation in Materials: Application to the "CO Adsorption Puzzle' and Other Systems. *Phys. Rev. Lett.* **2007**, *98*, 176103.

(6) Schimka, L.; Harl, J.; Stroppa, A.; Grüneis, A.; Marsman, M.; Mittendorfer, F.; Kresse, G. Accurate surface and adsorption energies from many-body perturbation theory. *Nat. Mater.* **2010**, *9*, 741−744.

(7) Gautier, S.; Steinmann, S. N.; Michel, C.; Fleurat-Lessard, P.; Sautet, P. Molecular adsorption at Pt(111). How accurate are DFT functionals? *Phys. Chem. Chem. Phys.* **2015**, *17*, 28921−28930.

(8) Fischer-Wolfarth, J. H.; Hartmann, J.; Farmer, J. A.; Flores-Camacho, J. M.; Campbell, C. T.; Schauermann, S.; Freund, H. J. An improved single crystal adsorption calorimeter for determining gas adsorption and reaction energies on complex model catalysts. *Rev. Sci. Instrum.* **2011**, *82*, 024102.

(9) Ertl, G.; Neumann, M.; Streit, K. M. Chemisorption of CO on the Pt(111) surface. *Surf. Sci.* **1977**, *64*, 393−410.

(10) Steininger, H.; Lehwald, S.; Ibach, H. On the adsorption of CO on Pt(111). *Surf. Sci.* **1982**, *123*, 264−282.

(11) Papp, C.; Steinrück, H.-P. In situ high-resolution X-ray photoelectron spectroscopy − Fundamental insights in surface reactions. *Surf. Sci. Rep.* **2013**, *68*, 446−487.

(12) Kinne, M.; Fuhrmann, T.; Whelan, C. M.; Zhu, J. F.; Pantförder, J.; Probst, M.; Held, G.; Denecke, R.; Steinrück, H.-P. Kinetic parameters of CO adsorbed on Pt(111) studied by in situ high resolution x-ray photoelectron spectroscopy. *J. Chem. Phys.* **2002**, *117*, 10852−10859.

(13) Hopster, H.; Ibach, H. Adsorption of CO on Pt(111) and Pt 6(111) × (111) studied by high resolution electron energy loss spectroscopy and thermal desorption spectroscopy. *Surf. Sci.* **1978**, *77*, 109−117.

(14) Heyden, B. E.; Bradshaw, A. M. The adsorption of CO on Pt(111) studied by infrared reflection—Absortion spectroscopy. *Surf. Sci.* **1983**, *125*, 787−802.

(15) Tüshaus, M.; Schweizer, E.; Hollins, P.; Bradshaw, A. M. Yet another vibratonal study of the adsorption system Pt{111}-CO. *J. Electron Spectrosc. Relat. Phenom.* **1987**, *44*, 305−316.

(16) Lahee, A. M.; Toennies, J. P.; Wöll, C. Low energy adsorbate vibrational modes observed with inelastic helium atom scattering: CO on Pt(111). *Surf. Sci.* **1986**, *177*, 371−388.

(17) Björneholm, O.; Nilsson, A.; Tillborg, H.; Bennich, P.; Sandell, A.; Hernnäs, B.; Puglia, C.; Mårtensson, N. Overlayer structure from adsorbate and substrate core level binding energy shifts: CO, CCH3 and O on Pt(111). *Surf. Sci.* **1994**, *315*, L983−L989.

(18) Thiel, P. A.; Williams, E. D.; Yates, J. T., Jr; Weinberg, W. H. The chemisorption of CO on Rh(111). *Surf. Sci.* **1979**, *84*, 54−64.

(19) Lauterbach, J.; Boyle, R. W.; Schick, M.; Mitchell, W. J.; Meng, B.; Weinberg, W. H. The adsorption of CO on Ir(111) investigated with FT-IRAS. *Surf. Sci.* **1996**, *350*, 32−44.

(20) Papp, H. The chemisorption of carbon monoxide on a Co(0001) single crystal surface; studied by LEED, UPS, EELS, AES and work function measurements. *Surf. Sci.* **1983**, *129*, 205−218.

(21) Pfnür, H.; Menzel, D.; Hoffmann, F. M.; Ortega, A.; Bradshaw, A. M. High resolution vibrational spectroscopy of CO on Ru(001): The importance of lateral interactions. *Surf. Sci.* **1980**, *93*, 431−452.

(22) Dion, M.; Rydberg, H.; Schröder, E.; Langreth, D. C.; Lundqvist, B. I. Van der Waals density functional for general geometries. *Phys. Rev. Lett.* **2004**, *92*, 246401.

(23) Klimeš, J.; Bowler, D. R.; Michaelides, A. Van der Waals density functionals applied to solids. *Phys. Rev. B: Condens. Matter Mater. Phys.* **2011**, *83*, 195131.

(24) Perdew, J. P.; Burke, K.; Ernzerhof, M. Generalized Gradient Approximation Made Simple. *Phys. Rev. Lett.* **1996**, *77*, 3865.

(25) Wellendorff, J.; Lundgaard, K. T.; Møgelhøj, A.; Petzold, V.; Landis, D. D.; Nørskov, J. K.; Bligaard, T.; Jacobsen, K. W. Density functionals for surface science: Exchange-correlation model development with Bayesian error estimation. *Phys. Rev. B: Condens. Matter Mater. Phys.* **2012**, *85*, 235149.

(26) Kresse, G.; Furthmüller, J. Efficient iterative schemes for ab initio total-energy calculations using a plane-wave basis set. *Phys. Rev. B: Condens. Matter Mater. Phys.* **1996**, *54*, 11169.

(27) Kresse, G.; Furthmüller, J. Efficiency of ab-initio total energy calculations for metals and semiconductors using a plane-wave basis set. *Comput. Mater. Sci.* **1996**, *6*, 15.

(28) Weinhold, F.; Landis, C. *Valency and Bonding—A Natural Bond Orbital Donor-Acceptor Perspective*; Cambridge University Press: Cambridge, 2005; pp 1−44.

(29) Dunnington, B. D.; Schmidt, J. R. Generalization of Natural Bond Orbital Analysis to Periodic Systems: Applications to Solids and Surfaces via Plane-Wave Density Functional Theory. *J. Chem. Theory Comput.* **2012**, *8*, 1902−1911.

(30) Dronskowski, R.; Bloechl, P. E. Crystal orbital Hamilton populations (COHP): energy-resolved visualization of chemical bonding in solids based on density-functional calculations. *J. Phys. Chem.* **1993**, *97*, 8617−8624.

(31) Deringer, V. L.; Tchougréeff, A. L.; Dronskowski, R. Crystal Orbital Hamilton Population (COHP) Analysis As Projected from Plane-Wave Basis Sets. *J. Phys. Chem. A* **2011**, *115*, 5461−5466.

(32) Bader, R. F. W. *International Series of Monographs on Chemistry*; Oxford University Press: Oxford, 1990; Vol. 22, pp 5−6.

(33) Gunasooriya, G. T. K. K.; van Bavel, A. P.; Kuipers, H. P. C. E.; Saeys, M. CO adsorption on cobalt: Prediction of stable surface phases. *Surf. Sci.* **2015**, *642*, L6−L10.

(34) Gunasooriya, G. T. K. K.; van Bavel, A. P.; Kuipers, H. P. C. E.; Saeys, M. Key Role of Surface Hydroxyl Groups in C−O Activation during Fischer−Tropsch Synthesis. *ACS Catal.* **2016**, *6*, 3660−3664.

(35) Weststrate, C. J.; van de Loosdrecht, J.; Niemantsverdriet, J. W. Spectroscopic insights into cobalt-catalyzed Fischer−Tropsch synthesis: A review of the carbon monoxide interaction with single crystalline surfaces of cobalt. *J. Catal.* **2016**, *342*, 1−16.

(36) Blyholder, G. Molecular Orbital View of Chemisorbed Carbon Monoxide. *J. Phys. Chem.* **1964**, *68*, 2772−2777.

(37) Sung, S. S.; Hoffmann, R. How carbon monoxide bonds to metal surfaces. *J. Am. Chem. Soc.* **1985**, *107*, 578−584.

(38) van Santen, R. A.; Neurock, M. *Molecular Heterogeneous Catalysis*; Wiley-VCH Verlag GmbH & Co. KGaA: Weinheim, 2007; pp 83−160.

(39) Nilsson, A.; Pettersson, L. G. M. Chemical bonding on surfaces probed by X-ray emission spectroscopy and density functional theory. *Surf. Sci. Rep.* **2004**, *55*, 49−167.

(40) Crabtree, R. H. *The Organometallic Chemistry of the Transition Metals*; John Wiley & Sons, Inc.: Hoboken, NJ, 2005; pp 1−28.

(41) Liu, P.; Qin, R.; Fu, G.; Zheng, N. Surface Coordination Chemistry of Metal Nanomaterials. *J. Am. Chem. Soc.* **2017**, *139*, 2122−2131.

(42) Chua, Y. P. G.; Gunasooriya, G. T. K. K.; Saeys, M.; Seebauer, E. G. Controlling the CO oxidation rate over Pt/TiO2 catalysts by defect engineering of the TiO2 support. *J. Catal.* **2014**, *311*, 306−313.

(43) Gunasooriya, G. T. K. K.; Seebauer, E. G.; Saeys, M. Ethylene Hydrogenation over Pt/TiO2: A Charge-Sensitive Reaction. *ACS Catal.* **2017**, *7*, 1966−1970.

(44) Gunasooriya, G. T. K. K.; Saeys, M. *Nanotechnology in Catalysis*; Wiley-VCH Verlag GmbH & Co. KGaA: Weinheim, 2017; pp 209−224.

(45) Ertl, G. Surface Science and Catalysis—Studies on the Mechanism of Ammonia Synthesis: The P. H. Emmett Award Address. *Catal. Rev.: Sci. Eng.* **1980**, *21*, 201−223.

(46) Strongin, D. R.; Somorjai, G. A. The effects of potassium on ammonia synthesis over iron single-crystal surfaces. *J. Catal.* **1988**, *109*, 51−60.